



## Spectroscopic detection of COClF in the tropical and mid-latitude lower stratosphere

Curtis P. Rinsland<sup>a,\*</sup>, Ray Nassar<sup>b</sup>, Chris D. Boone<sup>c</sup>, Peter Bernath<sup>c,1</sup>,  
Linda Chiou<sup>d</sup>, Debra K. Weisenstein<sup>e</sup>, Emmanuel Mahieu<sup>f</sup>, Rodolphe Zander<sup>f</sup>

<sup>a</sup>NASA Langley Research Center, Science Directorate, Mail Stop 401A, Hampton, VA 23681-2199, USA

<sup>b</sup>Department of Earth and Planetary Sciences, Division of Engineering and Applied Sciences, Harvard University, Pierce Hall, 107F, 29  
Oxford St., Cambridge, MA 02138, USA

<sup>c</sup>Department of Chemistry, University of Waterloo, Waterloo, Ont., Canada N2L 3G1

<sup>d</sup>Science Applications International Corporation, Enterprise Parkway, Mail Stop 927, Hampton, VA 23666, USA

<sup>e</sup>Atmospheric and Environmental Research, Inc., Lexington, MA 02421, USA

<sup>f</sup>Institute of Astrophysics and Geophysics, University of Liège, Liège, Belgium

Received 31 August 2006; received in revised form 7 November 2006; accepted 14 November 2006

### Abstract

We report retrievals of COClF (carbonyl chlorofluoride) based on atmospheric chemistry experiment (ACE) solar occultation spectra recorded at tropical and mid-latitudes during 2004–2005. The COClF molecule is a temporary reservoir of both chlorine and fluorine and has not been measured previously by remote sensing. A maximum COClF mixing ratio of  $99.7 \pm 48.0$  pptv ( $10^{-12}$  per unit volume, 1 sigma) is measured at 28 km for tropical and subtropical occultations (latitudes below  $20^\circ$  in both hemispheres) with lower mixing ratios at both higher and lower altitudes. Northern hemisphere mid-latitude mixing ratios ( $30$ – $50^\circ\text{N}$ ) resulted in an average profile with a peak mixing ratio of  $51.7 \pm 32.1$  pptv, 1 sigma, at 27 km, also decreasing above and below that altitude. We compare the measured average profiles with the one reported set of in situ lower stratospheric mid-latitude measurements from 1986 and 1987, a previous two-dimensional (2-D) model calculation for 1987 and 1993, and a 2-D-model prediction for 2004. The measured average tropical profile is in close agreement with the model prediction; the northern mid-latitude profile is also consistent, although the peak in the measured profile occurs at a higher altitude (2.5–4.5 km offset) than in the model prediction. Seasonal average 2-D-model predictions of the COClF stratospheric distribution for 2004 are also reported.

© 2006 Elsevier Ltd. All rights reserved.

**Keywords:** Remote sensing; Stratospheric chemistry; Infrared atmospheric remote sounding; Measurement–model comparisons; Stratospheric chlorine chemistry; Stratospheric fluorine chemistry

\*Corresponding author. Tel.: +1 7578642699; fax: +1 7578648197.

E-mail addresses: c.p.rinsland@larc.nasa.gov (C.P. Rinsland), ray@io.harvard.edu (R. Nassar), cboone@acebox.uwaterloo.ca (C.D. Boone), bernath@uwaterloo.ca (P. Bernath), l.s.chiou@larc.nasa.gov (L. Chiou), dweisens@aer.com (D.K. Weisenstein), Emmanuel.-Mahieu@ulg.ac.be (E. Mahieu), R.Zander@ulg.ac.be (R. Zander).

<sup>1</sup>Current address: Department of Chemistry, University of York, Heslington, York YO10 5DD, UK.

## 1. Introduction

There now exists evidence from ground-based solar absorption spectra, model calculations, and solar occultation measurements that chlorine loading is near its maximum in the lower stratosphere and it is expected to slowly decline with time [1–4]. However, because of the crucial role of chlorine in ozone loss and possible climate-induced changes in atmospheric chemistry [5], there remains a need to monitor stratospheric chlorine and improve methods for quantification of chlorine and fluorine chemistry from both ground-based and space-based observations. Infrared measurements covering nearly all components of the chlorine and fluorine budgets (with a few exceptions) can be retrieved directly from high-resolution solar occultation spectra [6–10], and hence such observations are needed for verification of model chemistry and for prediction of future trends.

One halogen-bearing molecule not yet derived from infrared remote sensing measurements is COClF. Carbonyl chlorofluoride or chlorofluorocarbonyl (COClF), also referred to as CFCIO or OCCIF, is a reservoir species that results from the breakdown of  $\text{CCl}_3\text{F}$  [6–13]. It is the most easily photolyzed F-containing breakdown product with a mixing ratio that decreases rapidly above the peak. Modeled COClF assuming a 3% per year increase between 1990 and 1994 was used to estimate stratospheric chlorine from Atmospheric Trace MOlecule Spectroscopy (ATMOS) measurements at northern mid-latitudes (35–49°N) and the northern subtropics during 1994 [13]. Production of COClF is analogous to the  $\text{CH}_4$  oxidation scheme, and is based on the assumption that in chlorofluorocarbons (CFCs), all C–Cl bonds break before C–F bonds and for HCFCs, C–H bonds break first, followed by C–Cl bonds, and then C–F bonds. This implies that  $\text{CCl}_2\text{F}_2$  will breakdown to form  $\text{COF}_2$  and that  $\text{CCl}_3\text{F}$  will breakdown to form COClF as follows:



Removal of COClF by  $\text{O}(^1\text{D})$  was also accounted for with the modeled COClF distribution reported as a function of latitude and different seasons in 1989 [13].

The global distribution of COClF [13] for 1989 was predicted to be relatively symmetric about the equator with the highest VMR of  $\sim 100$  pptv (1 pptv =  $10^{-12}$  per unit volume) at 20 hPa. The model distribution showed lower maximum VMRs with peaks shifted to higher pressure levels in both hemispheres for March and June 1989. Photolysis causes the reduction at higher altitudes with only a very small COClF seasonal variation predicted. Both chlorine and fluorine atoms are contained in COClF with loadings that have changed with time, but to our knowledge, no recent model COClF predictions or measurements of COClF loadings have been reported.

The purpose of this paper is to describe the analysis of infrared solar occultation spectra recorded by the atmospheric chemistry experiment (ACE) Fourier transform spectrometer (FTS) [14] for COClF concentrations in the lower stratosphere. Absorption by COClF is very weak even in the high-resolution ACE spectra, so we report averages of retrievals from spectra recorded during 2004 and 2005 at tropical-subtropical (20°S–20°N) and northern mid-latitudes (30–50°N). The retrieved profiles for both latitude bands are plotted against two-dimensional (2-D) model calculations for the same time period and are compared with previous model predictions, the single reported measurement set obtained during northern mid-latitude aircraft flights sampling the upper troposphere and lower stratosphere in 1986 and 1987 [15], and model predictions for the ACE measurement time period.

## 2. Measurements

The ACE payload, also known as SCISAT-1, was successfully launched on 12 August 2003 into a 74° inclined orbit by a NASA-supplied Pegasus XL at 650 km altitude [13]. This small Canadian-designed and built satellite contains three instruments with a shared field of view, and with the primary goal of recording

high-resolution atmospheric spectra taking advantage of the high precision of the solar occultation technique. The infrared instrument is an FTS that records solar spectra below altitudes of 150 km at a spectral resolution of  $0.02\text{ cm}^{-1}$  (maximum optical path difference of  $\pm 25\text{ cm}$ ) with a  $1.25\text{ mrad}$  diameter field of view. The spectral cover  $750\text{--}4400\text{ cm}^{-1}$  and are analyzed unapodized to take full advantage of the high spectral resolution. The instrument is self-calibrating as low Sun solar occultation spectra are divided by exoatmospheric spectra from the same occultation. The ACE orbit yields tropical to high-latitude occultations in both hemispheres with a  $3\text{--}4\text{ km}$  vertical resolution. Additional instruments onboard SCISAT-1 are measurement of aerosol extinction in the stratosphere and troposphere by occultation (MAESTRO), a two channel UV-visible spectrophotometer, and two imagers with optical filters at  $0.525$  and  $1.02\text{ }\mu\text{m}$  to provide extinction from analysis of solar disk images.

### 3. Analysis and comparison with model predictions

Very limited information has been reported on the infrared spectrum of COCIF. A spectrum of the strong infrared COCIF  $\nu_1$  fundamental band at  $1876\text{ cm}^{-1}$  covering  $1790\text{--}1910\text{ cm}^{-1}$  recorded at  $0.02\text{ cm}^{-1}$  resolution was reported in an atlas of infrared laboratory spectra [16]. The atlas spectrum shows a series of prominent P-branch features at  $1860\text{--}1870\text{ cm}^{-1}$ , a Q branch at  $1875.8\text{ cm}^{-1}$ , and R-branch transitions extending to  $1890\text{ cm}^{-1}$ . Our study focuses on ACE solar occultation measurements obtained in the tropical–subtropical region and at northern mid-latitudes during 2004 and 2005. We base our analysis on COCIF line parameters from the ATMOS supplemental list [17,18]. That list covers two regions with parameters for the  $\nu_1$  band extending from  $1850.078$  to  $1907.929\text{ cm}^{-1}$ . Those parameters were added in the 1995 compilation [18]. Line intensities are described as very crude with a reported uncertainty of a factor of 3. All lines have a lower state energy of  $345.0\text{ cm}^{-1}$ , and an air-broadening coefficient of  $0.1\text{ cm}^{-1}\text{ atm}^{-1}$  at  $296\text{ K}$  with  $T^{-0.75}$  assumed for the coefficient of the temperature dependence of the air-broadening coefficient, where  $T$  is the temperature. The laboratory spectra were measured at room temperature at high spectral resolution. More recently, an analysis of the 6 fundamental bands of the  $\text{CO}^{35}\text{CIF}$  isotopologue was reported based on spectra of both  $^{35}\text{Cl}$ -enriched and natural samples recorded between  $340$  and  $2000\text{ cm}^{-1}$  at better than  $0.0033\text{ cm}^{-1}$  spectral resolution [19]. Although the analysis did show the comparison of a measured and a simulated spectrum in selected regions of the  $\nu_1$  band, no intensity measurements were reported, and no linelist based on this work appears in public databases such as the HITRAN 2004 compilation [20]. We also were unable to find any other studies reporting intensities, and were unsuccessful in locating air-broadening coefficients or pressure-induced line shift coefficients for individual air-broadened lines of the  $\nu_1$  band.

The spectral fitting algorithm used in the present analysis retrieves simultaneous profiles for COCIF and interferences of all measurements over a pre-specified altitude range [21–23]. The retrieval approach is similar to the one adopted by ACE [24] and the method of Carlott [25]. It is based on nonlinear least squares fitting of spectra for the target molecule and interfering molecules. Our analysis combines the COCIF lines from the 1995 ATMOS supplemental linelist [18], the ACE solar spectra, and spectral parameters for other molecules from HITRAN 2004 [20] with the retrieved profiles of temperature, pressure, and tangent altitude for individual ACE occultations [24]. A refractive ray tracing program was used with the ACE-derived temperature profile and tangent heights to calculate airmass-weighted pressures, temperatures, and atmospheric ray paths for individual ACE occultations. The calculation of the COCIF rotational and vibration partition function [23] assumes vibrational band locations in close approximation to those reported in the more recent study [19].

Similar to other infrared experiments (e.g., [9,22,24,26–28]), a set of microwindows were selected for analysis. The 8 selected windows are reported in Table 1 with the interferences fitted in addition to COCIF in the retrievals. The list includes the Q branch at  $1875.8\text{ cm}^{-1}$ , though similar to predicted absorption COCIF in the other windows, it is near the noise level, even in the tropical lower stratosphere. The full set of target and interfering species was used to retrieve each occultation profile.

As the absorption by COCIF is very weak, several empirically selected parameters were used to exclude occultations with noisy measurements at one or more altitudes. A parameter was fitted to model the effective resolution to account for additional self-apodization that decreases the effective resolution of the instrument

Table 1  
Selected microwindows

Minimum (cm <sup>-1</sup> )	Maximum (cm <sup>-1</sup> )
1860.00	1860.70
1861.90	1863.20
1864.00	1864.60
1864.90	1866.00
1866.60	1867.00
1868.50	1869.10
1870.40	1870.75
1874.50	1875.40

Interferences fitted in the analysis were H<sub>2</sub>O, CO<sub>2</sub>, O<sub>3</sub>, N<sub>2</sub>O, and NO for all regions. Maximum altitude was set to 30 km for both tropical and mid-latitude occultations. Tropical occultations were fit with the minimum altitude set to 19 km and 17 km was selected as the minimum for mid-latitude occultations.

as a function of wavenumber [24]. Profiles containing mixing ratios with large uncertainties relative to the measured value were also discarded from the tropical measurement set.

Fig. 1 presents normalized measured and simulated solar spectra for a portion of the spectra range covered by ACE in the infrared. The interval was selected because it is near the maximum of the predicted absorption in the P branch of the  $\nu_1$  COCIF band, the strongest infrared band. A reference a priori COCIF mixing ratio distribution was selected to provide a spectral depth for the stronger COCIF spectral features similar to those measured in the average spectrum. The mean spectrum was obtained by averaging 655 spectra from 178 occultations with tangent heights between 20 and 26 km from measurements during 2004. Molecule-by-molecule simulations for COCIF and the most significant interferences are shown below. The parameter to model the effective resolution to account for additional self-apodization was not included in the simulations. As a consequence, the simulated line shape is narrower than in the measured coadded spectrum with ringing noticeable for the stronger simulated lines. The measured and simulated spectra illustrate the complexity of the absorption in the region. Additionally, as strong solar CO lines occur in the COCIF  $\nu_1$  band region, it was necessary to avoid intervals containing strong solar CO lines in the exoatmospheric average spectrum because of minor imperfections in the cancelation of those features in the ratioed spectrum used in the retrievals. A similar procedure of ratioing low to exoatmospheric spectra was used previously in the analysis of ATMOS spectra solar occultation spectra [23].

Tropical measurements recorded during February, April, August, October, and December in 2004 and February and April 2005, and northern mid-latitude measurements from February, March, April, June, July, August, September, and December of 2004 and March, April, and May of 2005 were analyzed. Mean profiles were calculated for those two latitudinal regions with objective criteria used to exclude occultations based on the statistical uncertainty of the fit and a parameter to quantify the quality of the fit to the instrumental line shape. After exclusion of occultations with these objective criteria, 159 of the 321 tropical occultations were retained. Only data from 30 occultations of the available 337 at northern mid-latitudes were kept with similar criteria as applied for the tropical-subtropical occultations.

Fig. 2 presents two panel plots that show average spectra and residuals (measured minus calculated differences) derived from all ACE tropical spectra measurements in 2004 at latitudes between 20°S and 20°N and altitudes between 22 and 24 km. An average spectrum near 23 km was produced from 221 spectra. The selected spectral regions for the two intervals are located near the maximum of COCIF absorption in the P branch. Residuals obtained assuming the mean retrieved profile and those obtained with the COCIF mixing ratio set to zero at all altitudes are shown in the upper panel on an expanded scale. Asterisks mark the locations of significant differences corresponding to the locations of COCIF absorption lines. Interfering molecules fitted in the analysis were H<sub>2</sub>O, CO<sub>2</sub>, O<sub>3</sub>, N<sub>2</sub>O, and NO assuming the temperature profile and tangent height at 24 km inferred by the ACE version 2.2 software [24]. Similar comparisons with other windows near the COCIF absorption maximum also provide evidence for COCIF absorption in the ACE tropical spectra.

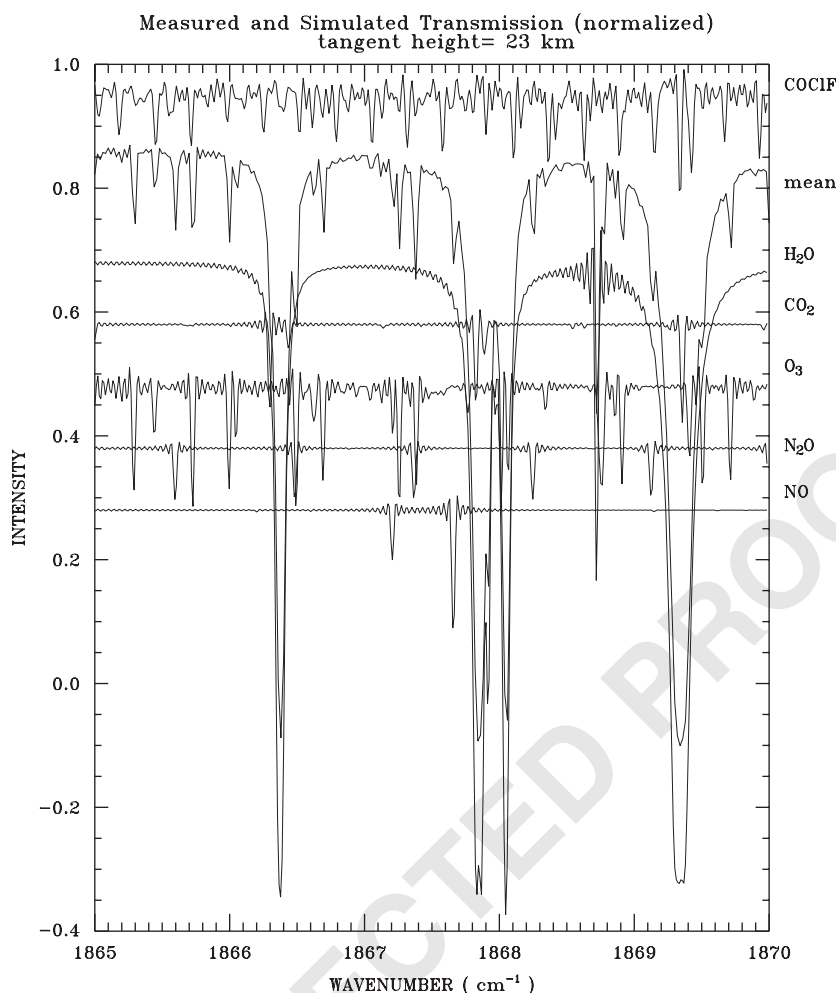


Fig. 1. Comparison of an average ACE tropical spectrum with molecule-by-molecule simulations for an altitude of 23 km. Spectra are normalized and offset vertically for clarity. As COClF is a weak absorber, a reference a priori mixing ratio profile has been scaled with a multiplicative factor to produce COClF spectral features with absorption depths similar to those in the measured tropical–subtropical average spectrum. The second spectrum is an average of 655 spectra from 178 occultations between latitudes of 20°S and 20°N and altitudes between 20 and 26 km during 2004.

The only reported lower stratospheric measurements of COClF were derived with the matrix isolation FTS technique [29] from measurements recorded during 5 aircraft flights in 1986 and 1987 between Germany and Spitzbergen (50–78°N) [14]. The mixing ratio of COClF was below the detection limit of 4 pptv at altitudes below the tropopause. A rapid increase of the COClF mixing ratios relative to the tropopause height was measured at higher altitudes increasing to  $18 \pm 5$  pptv at 5 km above the tropopause.

As measurements of COClF are so limited and previous model studies were for 1989 [13] and September 1993 [10], model calculations appropriate for the ACE measurement time were performed with the Atmospheric and Environmental Research, Inc. (AER) 2-D chemical-transport model [30–34]. As described in those previous studies, the AER model domain extends from the ground to 60 km with a vertical resolution of approximately 1.2 km and from pole to pole with horizontal resolution of 9.5°. Model temperatures and transport/circulation are prescribed according to climatology and do not respond to changes in aerosols or chemical species. The model includes full  $O_x$ ,  $HO_x$ ,  $CHO_x$ ,  $NO_x$ ,  $ClO_x$ , and  $BrO_x$  photochemistry. Loss of COClF is by photolysis and reaction with  $O(^1D)$  assuming JPL-2006 rates [35]. A surface boundary of 253.26 pptv for  $CCl_3F$  in 2004 was assumed. Production from  $CCl_3F$  total loss (photolysis and  $O(^1D)$ ) assumes COClF is immediately produced when  $CCl_3F$  reacts. Washout is parameterized as a first-order loss



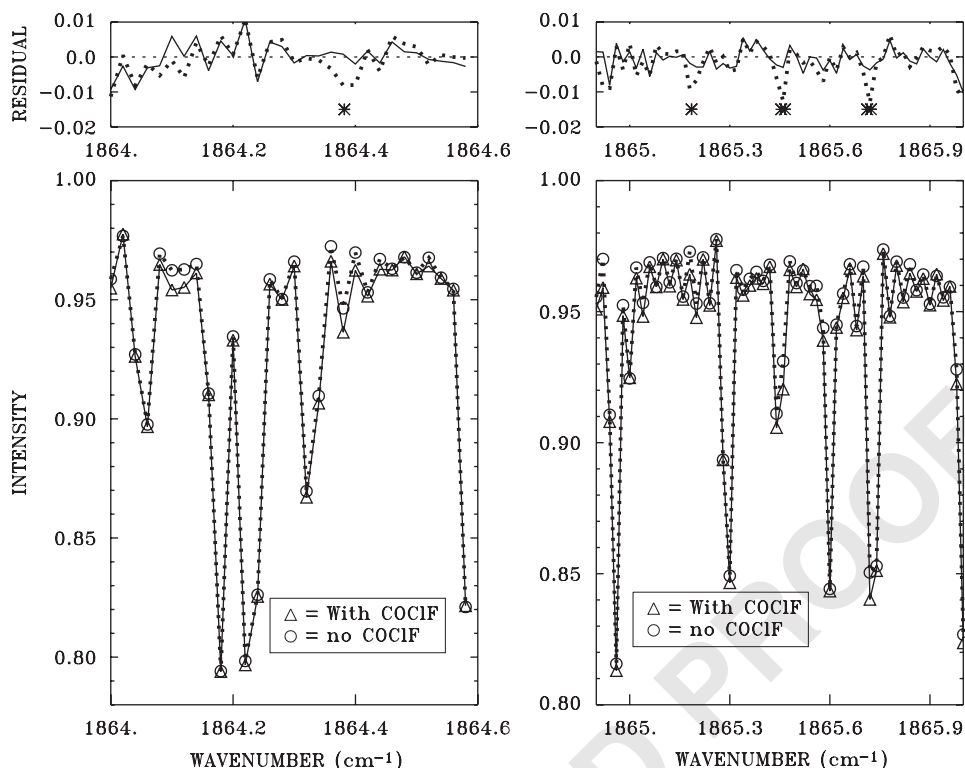


Fig. 2. Bottom panels: comparison of averages of all ACE tropical spectra measurements in 2004 at latitudes between 20°S and 20°N and altitudes between 22 and 24 km obtained with the best-fit COClF profile with those obtained assuming the COClF mixing ratio is zero at all altitudes. Upper panels: residuals (measured minus calculated signals) on an expanded vertical scale. Asterisks mark locations of stronger COClF features in the sample intervals.

rate below 10 km with a dependence on altitude as follows: 5 days for 0–2 km, 6.5 days at 2.9 km, 8 days at 4.0 km, 10 days at 5.2 km, 20 days at 6.4 km, 30 days at 7.6 km, and 40 days at 8.8–10 km. Tests run with the washout rate half or double of those values produce no changes in the stratosphere. A washout rate corresponding to a lifetime of 40 days up to the tropopause in the tropics made a 4% difference at 17 km and no difference above 20 km in the tropics.

Fig. 3 compares the ACE measurements for two latitude bands with the AER model predictions for 2004. The tropical measurements and model predictions both show an increase with altitude above 20 km with the measurements reaching a maximum mixing ratio of  $99.7 \pm 48.0$  pptv (1 sigma) at 28 km, declining rapidly above, very similar to the prediction for 1989 [10]. Mid-latitude mixing ratios (30–50°N) resulted in a profile with lower mixing ratios at all altitudes and a maximum VMR of  $51.7 \pm 32.1$  pptv, 1 sigma, at 27 km, consistent with the AER 2-D-model maximum although the model-predicted COClF mid-latitude peak is reached 3 km lower than that retrieved from the measurements. The AER model predictions for tropical and mid-latitudes also appear to be roughly consistent with those predicted for the 1989 northern mid-latitudes, but our measured mid-latitude maximum of  $51.7 \pm 32.1$  pptv is lower than the model-predicted September 1993 maximum of 83 pptv at 26 km [13]. However, there is consistency when considering the large statistical uncertainty of our mean profile measurement. Profile measurements above 30 km likely underestimate the precision as window selection was based on interferences at 18–30 km (Table 1) with absorption weaker than those in the coadded spectra illustrated in Figs. 1 and 2. Lower mixing ratios and large uncertainty at northern mid-latitudes make comparison of our result with the one set of mid-latitude COClF lower stratospheric measurements obtained within 5 km of the tropopause in 1986 and 1987 [15] difficult. However, their failure to detect COClF mixing ratios in the troposphere above the measurement uncertainty of 4 pptv provides evidence

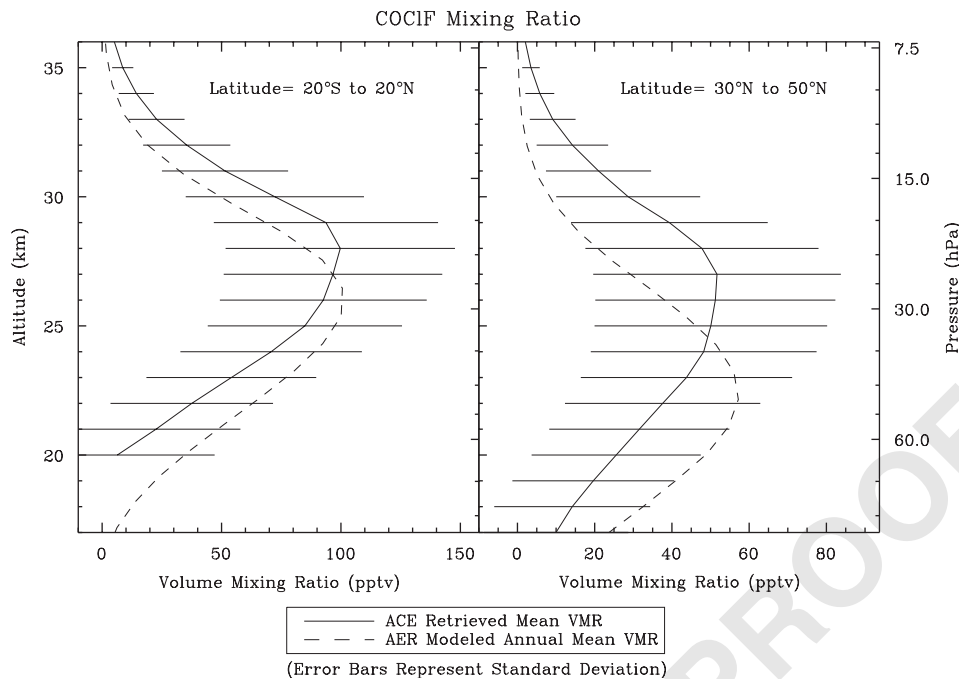


Fig. 3. Comparison of mean ACE COCIF mixing ratios vs. altitude for tropical latitudes (20°S–20°N) and northern mid-latitudes (30–50°N) from 2004 and 2005 with AER two-dimensional model calculations for 2004 (annual average). Horizontal error bars indicate standard deviations. Approximate pressures are indicated on the right vertical axis.

for the importance of tropospheric washout in the upper troposphere and the need for its inclusion in model predictions.

Fig. 4 presents the AER 2-D-model COCIF global distribution predicted as a function of season for 2004. The model shows a maximum in the tropical stratosphere with no significant seasonal variation, consistent with the higher tropical than mid-latitude maximum measured by ACE, the single set of 1986 and 1987 in situ measurements [15], and previously reported model predictions [10,13]. The AER global COCIF distribution for 2004 is close to a prediction by one of us (R. Nassar) obtained by scaling and vertically shifting the 2-D-model prediction for 1989 [13]. Latitude–height COCIF crosssections predicted for the month of December based on 1990 tropospheric source gas mixing ratios had a predicted peak mixing ratio of 0.11 ppbv in the tropical lower stratosphere [36] with tropospheric washout assumed, though details of the mechanism and pathway parameterization were not described.

#### 4. Summary and conclusions

We have reported spectroscopic evidence for lower to middle stratospheric carbonyl chlorofluoride (COCIF) from an analysis of ACE spectra at tropical–subtropical latitudes (20°S–20°N) and northern mid-latitudes (30–50°N) during 2004 and 2005. The results show mixing ratio profiles with maxima in the lower stratosphere for both latitude bands, consistent with AER 2-D-model calculations for 2004. Our results provide the first quantitative measurement of carbonyl chlorofluoride in the lower stratosphere. Our measured profiles are roughly consistent with predictions from similar models for 1989 [13] and September 1993 [10]. However, the uncertainties in our mean mid-latitude profile are too large to provide validation of the single reported set of northern hemisphere in situ measurements in the upper troposphere and lower stratosphere from 1986 and 1987 [15]. Although our analysis provides observational evidence for COCIF in the lower stratosphere, laboratory studies are needed to obtain accurate intensities, air-broadening coefficients, and air-

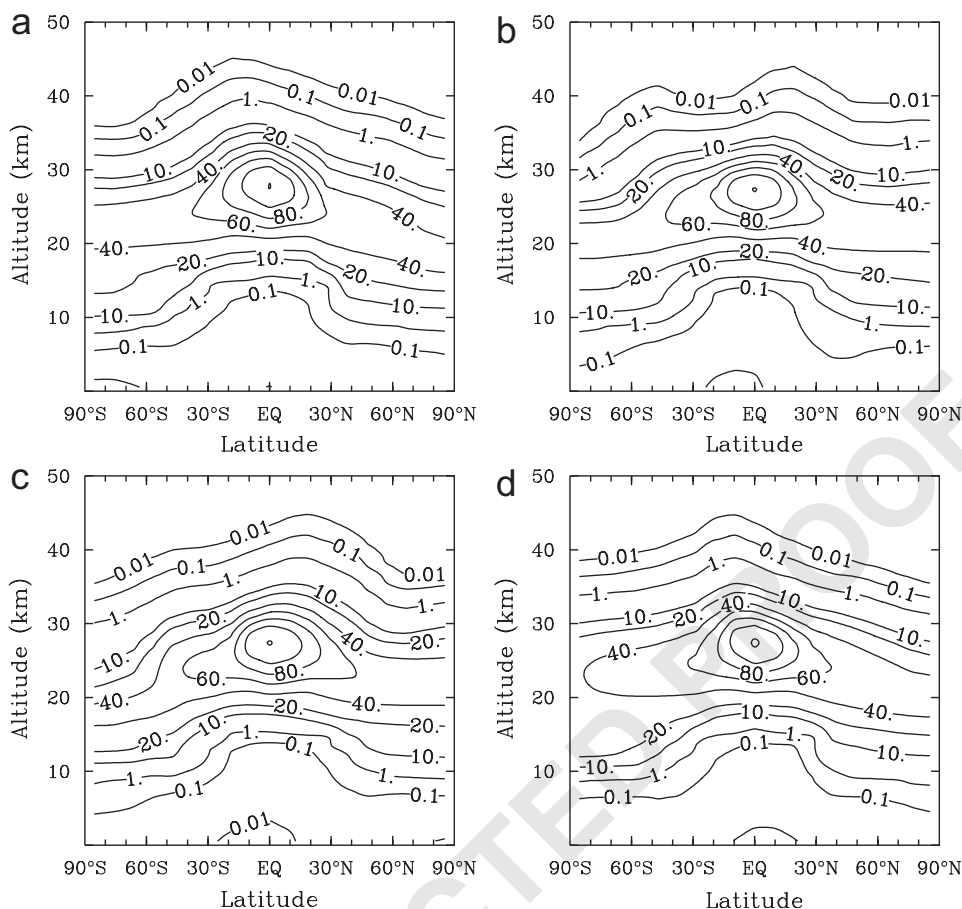


Fig. 4. COCIF global distribution for 2004 predicted by the AER 2-D model for (a) March, (b) June, (c) September, and (d) December in units of pptv.

induced pressure shift coefficients for lower stratospheric temperatures to reduce the large uncertainty in our measured profiles due to the limited precision and accuracy of the assumed spectroscopic parameters. Results are needed for the  $\nu_1$  band, the only one strong enough in the infrared for measurement over long atmospheric paths at high spectral resolution. Intensity measurements of the  $\nu_1$  band are recommended as the highest priority for laboratory studies because of the factor of three uncertainty in the ATMOS value.

## Acknowledgments

The investigation at the NASA Langley Research Center was supported by NASA's Upper Atmosphere Research Program and the Atmospheric Chemistry, Modeling, and Analysis Program (ACMAP). Funding for ACE is provided by the Canadian Space Agency and the Natural Sciences and Engineering Research (NSERC) Council of Canada. Support at Waterloo was also provided by the NSERC-Bomem-CSA-MSA Industrial Research Chair in Fourier Transform Spectroscopy. Research at AER was supported by ACPMAP. We thank Malcolm Ko of NASA Langley Research Center for comments on modeling, in particularly for noting the need for including washout in the model prediction.



## 1 References

- 3 [1] Mahieu E, Duchatelet P, Zander R, Demoulin P, Servais C, Rinsland CP, et al. The evolution of inorganic chlorine above the Jungfraujoch station: an update. In: Zerefos CS, editor. Ozone, vol. II. Proceedings of the XX quadrennial ozone symposium, Kos, Greece, 1–8 June 2004. p. 997–8.
- 5 [2] Rinsland CP, et al. Long-term trends in inorganic chlorine from ground-based infrared solar spectra: past increases and evidence for stabilization. *J Geophys Res* 2003;108(D8):4252.
- 7 [3] World Meteorological Organization. Scientific assessment of ozone depletion: 2002. Global ozone research and monitoring project—Report no. 47, Geneva, Switzerland, 2003.
- 9 [4] Rinsland CP, Boone C, Nassar R, Walker K, Bernath PF, Mahieu E, et al. Trends of HF, HCl, CCl<sub>2</sub>F<sub>2</sub>, CCl<sub>3</sub>F, CHClF<sub>2</sub> (HCFC-22) and SF<sub>6</sub> in the lower stratosphere from atmospheric chemistry experiment (ACE) and atmospheric trace molecule spectroscopy (ATMOS) measurement near 30°N latitude. *Geophys Res Lett* 2005;32:L16S03.
- 11 [5] Yang E-S, et al. Attribution of recovery in lower-stratospheric ozone. *J Geophys Res* 2007, in press.
- 13 [6] Zander R, Gunson MR, Farmer CB, Rinsland CP, Irion FW, Mahieu E. The 1985 chlorine and fluorine inventories in the stratosphere based on ATMOS observations at 30° North latitude. *J Atmos Chem* 1992;15:171–86.
- 15 [7] Zander R, et al. The 1994 northern midlatitude budget of stratospheric chlorine derived from ATMOS/ATLAS-3 observations. *Geophys Res Lett* 1996;23(17):2357–60.
- 17 [8] Nassar R, et al. A global inventory of stratospheric chlorine in 2004. *J Geophys Res* 2006, in press.
- 19 [9] Nassar R, Bernath PF, Boone CD, McLeod SD, Rinsland CP, Skelton R, et al. A global inventory of stratospheric fluorine in 2004 based on ACE-FTS measurements. *J Geophys Res* 2006, in press.
- 21 [10] Sen B, Toon GC, Blavier J-F, Fleming EL, Jackman CH. Balloon-borne observations of midlatitude fluorine abundance. *J Geophys Res* 1996;101:9045–54.
- 23 [11] Jayanty RKM, Simonaitis R, Heicklen J. The photolysis of chlorofluoromethanes in the presence of O<sub>2</sub> or O<sub>3</sub> at 213.9 nm and their reactions with O(<sup>1</sup>D). *J Photochem* 1975;4:381–98.
- 25 [12] Wu F, Carr RW. Time-resolved observation of the formation of CF<sub>2</sub>O and CFCIO in the CF<sub>2</sub>Cl + O<sub>2</sub> and CFCI<sub>2</sub> + O<sub>2</sub> reactions. The unimolecular elimination of Cl atoms from CF<sub>2</sub>ClO and CFCI<sub>2</sub>O radicals. *J Phys Chem* 1992;96:1743–8.
- 27 [13] Kaye JA, Douglass AR, Jackman CH, Stolarski RS, Zander R, Rowland G. Two-dimensional model calculation of fluorine-containing reservoir species in the stratosphere. *J Geophys Res* 1991;96:12865–81.
- 29 [14] Bernath PF, et al. Atmospheric chemistry experiment (ACE): mission overview. *Geophys Res Lett* 2005;32:L15S01.
- 31 [15] Wilson SR, Schuster G, Helas G. Measurements of COFCl and COCl<sub>2</sub> near the tropopause, In: Bojkov RD, Fabian P, editors. Ozone in the stratosphere. Proceedings of the quadrennial ozone symposium 1988 and tropospheric ozone workshop, 1989. p. 302–5.
- 33 [16] Murcray DG, Murcray FJ, Goldman A, Bonomo FS, Blatherwick RD. High resolution infrared laboratory spectra, Department of Physics, University of Denver, CO, USA, 1984.
- 35 [17] Brown LR, Farmer CB, Rinsland CP, Toth RA. Molecular line parameters for the atmospheric trace molecule spectroscopy experiment. *Appl Opt* 1987;26:5154–82.
- 37 [18] Brown LR, et al. 1995 atmospheric trace molecule spectroscopy (ATMOS) linelist. *Appl Opt* 1996;35:2828–48.
- 39 [19] Perrin A, Flaud J-M, Bürger H, Pawelke G, Sander S, Willner H. First high-resolution analysis of the six fundamental bands  $\nu_1$ ,  $\nu_2$ ,  $\nu_3$ ,  $\nu_4$ ,  $\nu_5$ , and  $\nu_6$  of COF<sup>35</sup>Cl in the 340–2000-cm<sup>-1</sup> region. *J Mol Spectrosc* 2001;209:122–32.
- 41 [20] Rothman LS, Jacquemart P, Barbe A, et al. The HITRAN 2004 molecular spectroscopic database. *JQSRT* 2005;96:139–204.
- 43 [21] Rinsland CP, Gunson MR, Foster JC, Toth RA, Farmer CB, Zander R. Stratospheric profiles of heavy water vapor isotopes and CH<sub>3</sub>D from analysis of the ATMOS Spacelab 3 infrared solar spectra. *J Geophys Res* 1991;96:1057–68.
- 45 [22] Rinsland CP, et al. ATMOS/ATLAS 3 infrared profile measurements of trace gases in the November 1994 tropical and subtropical upper troposphere. *JQSRT* 1998;5:891–901.
- 47 [23] Norton RH, Rinsland CP. ATMOS data processing and science analysis methods. *Appl Opt* 1991;30:389–400.
- 49 [24] Boone CD, Nassar R, Walker KA, Rochon Y, McLeod SD, Rinsland CP, et al. Retrievals for the atmospheric chemistry experiment Fourier-transform spectrometer. *Appl Opt* 2005;44:7218–31.
- 51 [25] Carlott M. Global-fit approach to the analysis of limb-scanning atmospheric measurements. *Appl Opt* 1988;27:3250–4.
- [26] von Clarmann T, Echle G. Selection of optimized microwindows for atmospheric spectroscopy. *Appl Opt* 1998;37(33):7661–9.
- [27] Irion FW, et al. The atmospheric trace molecule spectroscopy experiment (ATMOS) version 3 data retrievals. *Appl Opt* 2002;41:6968–79.
- [28] Rinsland CP, Luo M, et al. Nadir measurements of carbon monoxide (CO) distributions by the tropospheric emission spectrometer (TES) instrument onboard the aura spacecraft: overview of analysis approach and examples of initial results. *Geophys Res Lett* 2006, in press.
- [29] Griffith DWT, Schuster G. Atmospheric trace gas analysis using matrix isolation-Fourier transform infrared spectroscopy. *J Atmos Chem* 1987;5:59–81.
- [30] Shia R-L, Ko MKW, Weisenstein DK, Scott C, Rodriguez J. Transport between the tropical and mid-latitude lower stratosphere: implications for ozone response to high-speed civil transport emissions. *J Geophys Res* 1998;103:25435–46.
- [31] Weisenstein DK, Yue GK, Ko MKW, Sze N-D, Rodriguez JM, Scott CJ. A two-dimensional model of sulfur species and aerosols. *J Geophys Res* 1997;102:13019–35.
- [32] Weisenstein DK, Ko MKW, Dyominov IG, Pitari G, Ricciardulli L, Visconti G, et al. The effects of sulfur emissions from HSCT aircraft: a 2-D model intercomparison. *J Geophys Res* 1998;103:1527–47.

- 1 [33] Weisenstein DK, Eluszkiewicz J, Ko MKW, Scott CJ, Jackman CH, Fleming EL, et al. Separating chemistry and transport effects in  
two-dimensional models. *J Geophys Res* 2004;109:D18310.
- 3 [34] Rinsland CP, Weisenstein DK, Ko MKW, Scott CJ, Chiou LS, Mahieu E, et al. Post-Mount Pinatubo eruption ground-based  
infrared stratospheric column measurements of HNO<sub>3</sub>, NO, and NO<sub>2</sub> and their comparison with model calculations. *J Geophys Res*  
2003;108(D15):4437.
- 5 [35] Sander SP, et al. Chemical kinetics and photochemical data for use in atmospheric studies. JPL publication 06-02, Jet Propulsion  
Laboratory, Pasadena, CA, 2006. 522pp. Available at (<http://jpldataeval.jpl.nasa.gov/download.html>).
- 7 [36] Chipperfield MP, et al. On the use of HF as a reference for the comparison of stratospheric observations and models. *J Geophys Res*  
1997;102:12901–19.

UNCORRECTED PROOF